Fundamental bounds on decay rates in asymmetric single-mode optical resonators

Ken Xingze Wang,[1] Zongfu Yu,[2] Sunil Sandhu,[2] and Shanhui Fan[2,*]

[1]*Department of Applied Physics, Stanford University, Stanford, California 94305, USA*

[2]*Department of Electrical Engineering, Stanford University, Stanford, California 94305, USA*

**Corresponding author: shanhui@stanford.edu*

Received November 9, 2012; accepted December 2, 2012;
posted December 6, 2012 (Doc. ID 179549); published January 7, 2013

We derive tight upper and lower bounds of the ratio between decay rates to two ports from a single resonance exhibiting Fano interference, based on a general temporal coupled-mode theory formalism. The photon transport between these two ports involves both direct and resonance-assisted contributions, and the bounds depend only on the direct process. The bounds imply that, in a lossless system, full reflection is always achievable at Fano resonance, even for structures lacking mirror symmetries, while full transmission can only be seen in a symmetric configuration where the two decay rates are equal. The analytic predictions are verified against full-field electromagnetic simulations. © 2013 Optical Society of America

OCIS codes: 230.5750, 230.5298.

The properties of optical resonances [1–9], such as guided resonance in photonic crystal slabs [10–19], can be described by the temporal coupled-mode theory model shown in Fig. 1. A special case of the model consists of a resonator coupled to two ports with external coupling rates $1/\tau_1$ and $1/\tau_2$, respectively. In addition, the two ports may couple directly as a background process in the absence of the resonance. Such simultaneous presence of the direct (i.e., background) and the indirect (i.e., resonance-mediated) pathways gives rise to the Fano interference [13,20].

If the structure is asymmetric with respect to its midplane [see, for example, the photonic crystal slab structure in Fig. 2(a)], τ_1 and τ_2 could be different. In this Letter, we show that the ratio between τ_1 and τ_2 is constrained as follows by the direct process of the photon transport:

$$\frac{1-r}{1+r} \le \frac{\tau_1}{\tau_2} \le \frac{1+r}{1-r}, \tag{1}$$

where r is the amplitude reflection coefficient of the direct process. This inequality implies the existence of perfect reflection in the vicinity of the Fano resonance for arbitrarily asymmetric structures.

To prove Eq. (1), we start by reviewing the temporal coupled-mode theory model of Fig. 1. In this model, the dynamics of the resonance-mode amplitude u is described by

$$\frac{du}{dt} = \left(j\omega_0 - \frac{1}{\tau_1} - \frac{1}{\tau_2}\right)u + \begin{pmatrix} d_1 & d_2 \end{pmatrix}\begin{pmatrix} s_{1+} \\ s_{2+} \end{pmatrix}, \tag{2}$$

$$\begin{pmatrix} s_{1-} \\ s_{2-} \end{pmatrix} = C\begin{pmatrix} s_{1+} \\ s_{2+} \end{pmatrix} + \begin{pmatrix} d_1 \\ d_2 \end{pmatrix}u, \tag{3}$$

where $|u|^2$ corresponds to the electromagnetic energy in the resonance; ω_0 is the center frequency of the resonance; $1/\tau_1 + 1/\tau_2 = 1/\tau$ is the total decay rate, assuming that the resonance decays into the two ports with decay rates $1/\tau_1$ and $1/\tau_2$, respectively; s_{1+} and s_{2+} are the amplitudes of the incoming waves from the two ports; s_{1-} and s_{2-} are the amplitudes of the outgoing waves; and d_1 and d_2 are the coupling coefficients between the ports and the resonance. In addition to the resonance-assisted photon transport, the incoming and outgoing waves may also couple directly, as described by the direct-transport scattering matrix

$$C = e^{j\phi}\begin{pmatrix} r & jt \\ jt & r \end{pmatrix}, \tag{4}$$

where ϕ is a phase factor depending on the positions of the reference planes (dashed lines in Fig. 1), and r and t, both being real, are the reflection and transmission coefficients of the direct process satisfying $r^2 + t^2 = 1$.

According to energy conservation and time-reversal symmetry [13], the coupling coefficients satisfy

$$d_1^* d_1 = \frac{2}{\tau_1}, \qquad d_2^* d_2 = \frac{2}{\tau_2}, \tag{5}$$

$$C\begin{pmatrix} d_1 \\ d_2 \end{pmatrix}^* = -\begin{pmatrix} d_1 \\ d_2 \end{pmatrix}. \tag{6}$$

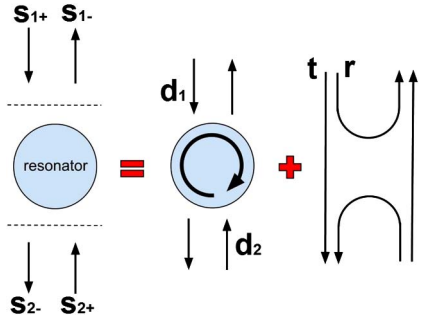

Fig. 1. (Color online) Schematic of a single resonance coupled to two ports. The amplitude of an output electromagnetic wave, either reflected or transmitted, is the sum of an indirect (resonance-assisted) component and a direct (background) component.

The formalism above is general. In [13], these equations were applied to symmetric structures where $1/\tau_1 = 1/\tau_2$. Here we consider the more general asymmetric case where the decay rates $1/\tau_1$ and $1/\tau_2$ are not necessarily equal. From Eqs. (4) and (6), we have

$$d_1 = -e^{j\phi}(rd_1^* + jtd_2^*), \tag{7}$$

$$d_2 = -e^{j\phi}(jtd_1^* + rd_2^*). \tag{8}$$

Substituting Eq. (7) into Eq. (5), we could solve for d_2^* in terms of d_1^*:

$$d_2^* = -\frac{1}{jt}\left(e^{-j\phi}\frac{2}{\tau_1}\frac{1}{d_1^*} + rd_1^*\right). \tag{9}$$

Next, substituting Eqs. (8) and (9) into Eq. (5), we obtain

$$\frac{2}{\tau_2} = \frac{1}{jt}\left(e^{-j\phi}\frac{2}{\tau_1}\frac{1}{d_1^*} + rd_1^*\right)e^{j\phi}\left[jtd_1^* - \frac{r}{jt}\left(e^{-j\phi}\frac{2}{\tau_1}\frac{1}{d_1^*} + rd_1^*\right)\right]. \tag{10}$$

Rearranging the terms in Eq. (10), we get

$$\frac{\tau_1}{\tau_2} = 1 + 2\left(\frac{r}{t}\right)^2 + 2\frac{r}{t^2}\cos\phi', \tag{11}$$

where $\phi' = \phi - j\ln(d_1^*/d_1)$. $\phi' \in \mathbb{R}$ because d_1^*/d_1 has the form $e^{j\theta}$, where $\theta \in \mathbb{R}$. Consequently, the bound $-1 \le \cos\phi' \le 1$ gives the constraint on the ratio between the two decay rates, as in Eq. (1).

Equation (1) indicates that, in general, the ratio between the two decay rates cannot be arbitrarily specified but is rather constrained by the direct process. In particular, if $r = 0$, that is, the background transmission pathway has a 100% coefficient, then $\tau_1 = \tau_2$ even for structures that have apparent asymmetry. On the other hand, a large difference in decay rates can occur when the background reflection coefficient r is large.

The theoretical derivation above is applicable to any single-mode optical resonator system. To verify the validity of the theory, we compare the bound in Eq. (1) with first-principles simulations [21,22] of one type of optical resonance: the guided resonance in a photonic crystal slab. We consider the asymmetric structure in Fig. 2(a), which consists of two layers of slabs. The first layer is a photonic crystal slab consisting of a square lattice of air holes. The slab has a dielectric constant of 12 and a thickness of $0.1a$, where a is the lattice constant. Each air hole has a radius of $0.3a$. The second layer is identical to the slab in the first layer but without the air holes. This asymmetric structure exhibits guided resonances, as shown in the plot of its transmission spectrum in Fig. 2(b).

In order to test different asymmetric structures, we next vary the following parameters of the asymmetric structure in Fig. 2(a): the number of layers, the thicknesses of the layers, the shape and size of the periodic pattern, and the dielectric constants of the materials and their superstrate and substrate. For each of these

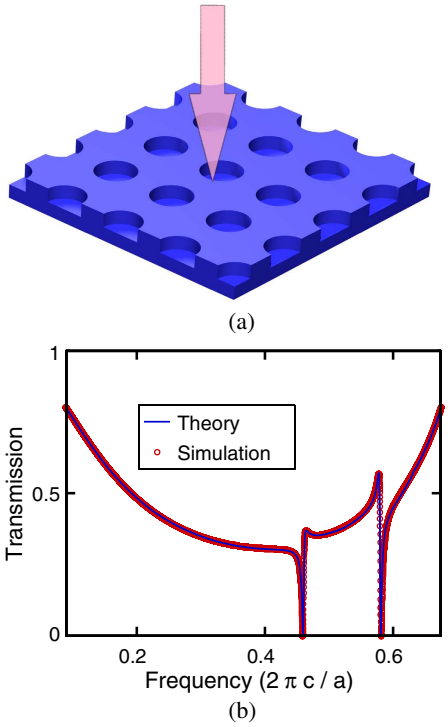

Fig. 2. (Color online) Asymmetric photonic crystal slab and its transmission spectrum. (a) Asymmetric photonic crystal slab structure consisting of two layers. The top layer has a square lattice of air holes of radius $0.3a$ introduced into a slab with dielectric constant 12 and thickness of $0.1a$, where a is the lattice constant. The bottom layer is a uniform slab of the same material and thickness. (b) Transmission spectra of the photonic crystal slab at normal incidence. The temporal coupled-mode theory results agree well with the simulation.

structures with varying geometries and materials, we calculate τ_1 or τ_2 of the resonance by studying the exponential temporal decay of the resonance amplitude after excitation. To establish the direct-scattering matrix C and in particular to determine the value of the background reflection coefficient r, we fit the transmission spectrum to a Fabry–Perot background, or a transmission spectrum of a uniform slab with an effective thickness and a frequency-dependent effective dielectric constant [11,13]. In Fig. 3, we plot the lifetime ratio versus reflection coefficient for 50 of the structures with r ranging from 0 to 1. All results fall between the theoretical bounds given in Eq. (1).

Similar to the symmetric case [13], we could analytically solve the coupled-mode equations to obtain the transmission or reflection spectra:

$$R = \frac{\left[r(\omega-\omega_0) \pm \sqrt{\frac{2}{\tau_1^2} + \frac{2}{\tau_2^2} - \left(\frac{r}{\tau}\right)^2 - \left(\frac{1}{r\sigma}\right)^2}\right]^2 + \left(\frac{1}{r\sigma}\right)^2}{(\omega-\omega_0)^2 + \left(\frac{1}{\tau}\right)^2}, \tag{12}$$

where $1/\tau = 1/\tau_1 + 1/\tau_2$ and $1/\sigma = 1/\tau_1 - 1/\tau_2$. Equation (12) is valid for any τ_1 and τ_2. Nonetheless, the bounds in Eq. (1) impose additional constraints on the value of R. In particular, for τ_1/τ_2 values within the bounds, zero transmission always occurs at

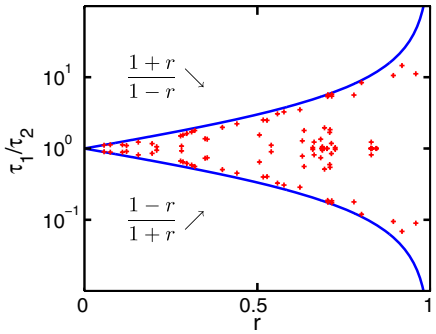

Fig. 3. (Color online) Scatterplot of the r and τ_1/τ_2 values of 50 different asymmetric photonic crystal slabs. (Each of the data points is reflected with respect to the line of $\tau_1 = \tau_2$ because the subscripts are interchangeable, and there are in total 100 scatter points in the plot.) r is obtained by fitting the simulated spectrum with a Fabry–Perot background characteristic of the direct process. τ_1/τ_2 is obtained by comparing the electromagnetic flux leaking above and below the structure.

$$\omega = \omega_0 \pm \frac{r}{1-r^2}\sqrt{\frac{2}{\tau_1^2}+\frac{2}{\tau_2^2}-r^2\left(\frac{1}{\tau_1}+\frac{1}{\tau_2}\right)^2-\frac{1}{r^2}\left(\frac{1}{\tau_1}-\frac{1}{\tau_2}\right)^2}. \tag{13}$$

As a result, we could design a perfect mirror with arbitrarily asymmetric single-mode resonators. This is in contrast to the Fabry–Perot resonance, where transmission could only approach zero at high finesse. We further note that the transmission maximum is $4\tau_1\tau_2/(\tau_1+\tau_2)^2$, which can only be unity at

$$\omega = \omega_0 \pm \frac{t}{r}\left(\frac{1}{\tau_1}+\frac{1}{\tau_2}\right)$$

and $\tau_1 = \tau_2$.

Finally, we compare the transmission spectra for the photonic crystal slab calculated by the coupled-mode theory result in Eq. (12) and by full-field electromagnetic simulation [21]. The simulation result, shown as circles in Fig. 2(b), consists of Fano resonance line shapes superimposed on a smooth Fabry–Perot background. Again, we determine from the simulations the frequency ω_0 and the widths $1/\tau_1$ and $1/\tau_2$ of each resonance and the frequency-dependent reflection coefficient r of the Fabry–Perot background. We then calculate the theoretical spectrum using Eq. (12) and plot it as a solid curve in Fig. 2(b). There is excellent agreement between theory and simulation. In particular, we note the lack of 100% transmission and the presence of 100% reflection [at frequencies given by Eq. (13)] for both resonances in this asymmetric configuration.

In conclusion, we analyzed the temporal coupled-mode theory for the single-resonance, double-port system. We found that the resonance-assisted pathway is restricted by the direct pathway in the sense that there exist tight bounds [Eq. (1)] on the ratio between the resonance decay rates into the two ports. These bounds have interesting consequences, such as the existence of total reflection in any single-mode resonance, and could serve as a guideline for controlling the proportionality of the energy decay into the two coupling ports of the system. The result can be a useful tool for designing resonance-based photonic devices with asymmetric structures. It would be of interest to extend this work to account for more complex situations involving multiple resonances and multiple ports [20,23].

This work is supported in part by DOE Grant No. DE-FG07-ER46426 and by the DOE Bay Area Photovoltaic Consortium. The simulations were performed on the NSF Extreme Science and Engineering Discovery Environment (XSEDE).

References

1. H. A. Haus, *Waves and Fields in Optoelectronics* (Prentice-Hall, 1984).
2. J. D. Joannopoulos, S. G. Johnson, J. N. Winn, and R. D. Meade, *Photonic Crystals: Molding the Flow of Light*, 2nd ed. (Princeton University, 2008).
3. S. Fan, *Optical Fiber Telecommunications V Vol. A: Components and Subsystems* (Elsevier, 2008), Chap. 12, p. 431.
4. H. Y. Song, S. Kim, and R. Magnusson, Opt. Express **17**, 23544 (2009).
5. Z. Yu, A. Raman, and S. Fan, Proc. Natl. Acad. Sci. USA **107**, 17491 (2010).
6. T. Lepetit, E. Akmansov, J.-P. Ganne, and J.-M. Lourtioz, Phys. Rev. B **82**, 195307 (2010).
7. H. Lu, X. Liu, Y. Gong, D. Mao, and L. Wang, Opt. Express **19**, 12885 (2011).
8. Z. Ruan and S. Fan, Phys. Rev. A **85**, 043828 (2012).
9. Y. Zhang, T. Mei, and D. Zhang, Appl. Opt. **51**, 504 (2012).
10. V. N. Astratov, I. S. Culshaw, R. M. Stevenson, D. M. Whittaker, M. S. Skolnick, T. F. Krauss, and R. M. De La Rue, J. Lightwave Technol. **17**, 2050 (1999).
11. S. Fan and J. D. Joannopoulos, Phys. Rev. B **65**, 235112 (2002).
12. S. G. Tikhodeev, A. L. Yablonskii, E. A. Muljarov, N. A. Gippius, and T. Ishihara, Phys. Rev. B **66**, 045102 (2002).
13. S. Fan, W. Suh, and J. D. Joannopoulos, J. Opt. Soc. Am. A **20**, 569 (2003).
14. Y. Ding and R. Magnusson, Opt. Express **12**, 5661 (2004).
15. A. Rosenberg, M. Carter, J. Casey, M. Kim, R. Holm, R. Henry, C. Eddy, V. Shamamian, K. Bussmann, S. Shi, and D. Prather, Opt. Express **13**, 6564 (2005).
16. M. Laroche, R. Carminati, and J.-J. Greffet, Phys. Rev. Lett. **96**, 123903 (2006).
17. Y. Kanamori, T. Kitani, and K. Hane, Appl. Phys. Lett. **90**, 031911 (2007).
18. M. Ghebrebrhan, P. Bermel, Y. X. Yeng, I. Celanovic, M. Soljacic, and J. D. Joannopoulos, Phys. Rev. A **83**, 033810 (2011).
19. H. Yang, D. Zhao, S. Chuwongin, J.-H. Seo, W. Yang, Y. Shuai, J. Berggren, M. Hammar, Z. Ma, and W. Zhou, Nat. Photonics **6**, 615 (2012).
20. W. Suh, Z. Wang, and S. Fan, IEEE J. Quantum Electron. **40**, 1511 (2004).
21. A. Taflove and S. C. Hagness, *Computational Electrodynamics: The Finite-Difference Time-Domain Method*, 3rd ed. (Artech House, 2005).
22. V. Liu and S. Fan, Comput. Phys. Commun. **183**, 2233 (2012).
23. M. Sumetskii and M. Felshtyn, J. Exp. Theor. Phys. Lett. **53**, 24 (1991).